MEASUREMENT ACCURACY IN NETWORK-RTK

RAGNE EMARDSON, PER JARLEMARK, JAN JOHANSSON, AND STEN BERGSTRAND

SP TECHNICAL RESEARCH INSTITUTE OF SWEDEN

MARTIN LIDBERG, AND BO JONSSON

LANTMÄTERIET

Abstract

New satellite systems such as the European Galileo and the ongoing modernization of GPS and GLONASS, allow for improvements in accurate positioning. Real Time Kinematic (RTK) is a system that utilises Global Navigation Satellite Systems (GNSS) to provide accurate positioning in real time. In this paper, we describe the error sources in network-RTK, and how the increased number of satellites and new signals are best served to achieve the desired improvement in performance. Using simulations we find that the inclusion of future satellite systems such as Galileo and Compass can reduce the error in the vertical coordinate of the estimated position from 27 mm to 20 mm for a reference network with 70 km between the reference stations. For periods with high spatial variability in the ionosphere, it is important to consider the tradeoff between influence from the ionosphere and from the local environment. A densified network with 35 km between the reference stations results in a similar improvement as the contribution of the new satellite systems. The error in the estimated vertical coordinate is reduced from 27 mm to 18 mm. Using both a densified network and the new satellite systems reduces the error further down to 13 mm.

Introduction

Real Time Kinematic (RTK) is a system that utilises Global Navigation Satellite Systems (GNSS) to provide accurate positioning in real time. The general idea in RTK is to receive GNSS-signals at a stationary reference with a known position and to use this information to correct measurement data at a roving receiver in another location. The ideal signal is perturbed by ionosphere, troposphere and imperfections related to ephemerides, clocks and multipath (historically also Selective Availability, SA) and thus the calculated position differs from the known. By calculating corrections that mathematically “moves” the reference to its known position and subsequently apply a similar set of corrections to the rover, the rover’s position can also be determined very accurately. As the reference and rover are at different locations, the signals have been perturbed differently and the correction data are therefore affected by uncertainties that compromise the reliability of the rover’s corrected position. The factors that affect the uncertainties can be classified in different ways, e.g. distance dependent, systematic, random, site specific, rapid, frequency dependent (dispersive).

With RTK it is also implicit that, in addition to the broadcast code signals that are handled by relatively cheap off-the-shelf products, the carrier phase of the signal is analysed with a geodetic type receiver. With this technique there is a potential for obtaining position coordinates with accuracies of the order of 1 cm. The difference between RTK and network-RTK is that the latter combines data from several reference stations to provide the rover with corrections. With network-RTK the distance dependent errors are interpolated between the reference stations, which allows for increased distance between reference stations without losing position accuracy. More on network-RTK can be found in e.g., *Landau et al*. [2002], *Rizos and Han*, [2003], *Lim and Rizos* [2008].

Background

In order to study the different error sources in network-RTK applications, we model the signal received by a single GNSS receiver. The phase observed by a rover (A) and a reference receiver (B) can be described by (1) and (2) respectively, where φ is the measured phase in fraction of cycles, λ is the signal wavelength, ρ is the true geometrical distance between the receiver and the satellite, N is the integer number of cycles referred to as the ambiguity parameter and f is the signal frequency. The δt^s and δt^r represent the satellite and receiver clock errors respectively, ℓ_o is the error in the reported satellite orbital model, ℓ_t is the signal delay in the lower part of the atmosphere referred to as the troposphere, ℓ_i is the signal delay in the ionosphere part of the atmosphere, μ is signal multipath, and ε is receiver measurement error.

$$\varphi_A = \frac{1}{\lambda}\rho_A + N_A + f\ (\delta t_A^s + \delta t_A^r) + \ell_{oA} + \ell_{iA} + \ell_{tA} + \mu_A + \varepsilon_A \quad (1)$$

$$\varphi_B = \frac{1}{\lambda}\rho_B + N_B + f\ (\delta t_B^s + \delta t_B^r) + \ell_{oB} + \ell_{iB} + \ell_{tB} + \mu_B + \varepsilon_B \quad (2)$$

Forming the difference between the observed signals at the rover and the reference stations, we obtain an observable, denoted with subscript *D*, that can be used for determining the vector between the rover and reference positions. By multiplying (1) and (2) with the signal wavelength and subtracting them, we obtain a phase difference measurement:

$$\lambda\varphi_D = \Delta\rho + c\delta t_D^s + \Delta\ell_o + \Delta\ell_i + \Delta\ell_t + c\delta t_D^r + \mu_D + \varepsilon_D \quad (3)$$

Here, we assume that the local integer ambiguities, *N*, are resolved. Hence, we can write the displacement range $\Delta\rho$ as:

$$\Delta\rho = \lambda\varphi_D - (c\delta t_D^t + c\delta t_D^r + \Delta\ell_o + \Delta\ell_i + \Delta\ell_t + \ell_e) \quad (4)$$

Where we have now combined the signal multipath, μ , and receiver measurement error, ε, into a local effect, ℓ_e

That is the sought displacement range equals the phase measurement difference including the errors in satellite clocks, local clocks, satellite orbits, delay in the ionosphere, delay in the troposphere, and local effects. Below, we describe the different error sources and explain how they influence the network-RTK position estimates.

Modelling Assumptions

We assess position estimation errors by mathematically studying the influence of the error sources presented above. We assume a network configuration as outlined in Figure 1. The distance, d_{ref}, between the reference stations is 70 km. When positioning a rover as depicted in Figure 1 as a blue circle, we assume the use of information from the surrounding reference stations. In our configuration, the use of measurements from six surrounding reference stations is simulated. Three of those form an inner triangle and the rest form an outer triangle.

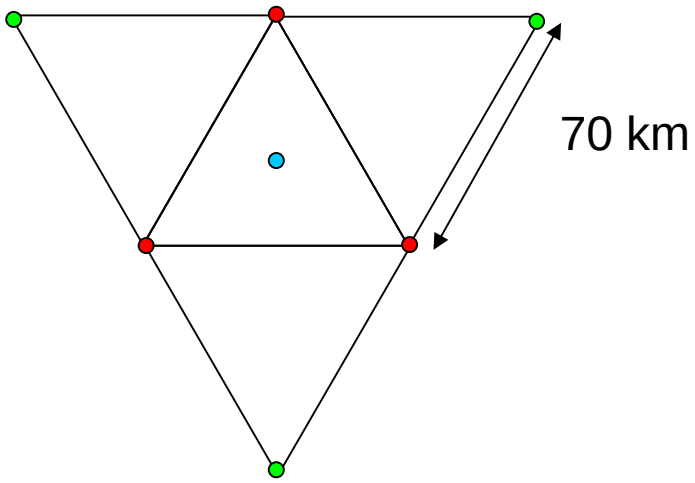

Figure 1 **Network configuration. The reference stations are shown in red (inner triangle) and green (outer triangle) and the rover is shown in blue.**

Here the distance from the rover to any reference station in the inner triangle is

$$d_a = d_{ref} / \sqrt{3} \tag{5}$$

and the distance from the rover to a reference station in the outer triangle is

$$d_b = 2 d_{ref} / \sqrt{3} \tag{6}$$

where in the nominal situation d_{ref} = 70km. Hence the interpolated phase, which constitutes a virtual reference station [*Landau et al*., 2002], at the site of the rover can be written as:

$$\varphi_r = \sum_i w_a \varphi_i + \sum_j w_b \varphi_j \tag{7}$$

Where we choose the weights w_a=2/9 and w_b=1/9 for the inner and outer reference station data respectively. This choice is a trade off between an optimal choice for atmospheric interpolation where we benefit from higher weights on the stations in the inner triangle and optimal choice for local effects where an optimal weighing would be w_a=w_b=1/6.

In forming (7) we assume that broadcast satellite positions and a priori atmospheric delay are removed from the phase observables before the summation above. We also assume that all *a priori* phase ambiguities are fixed to integer values. Ambiguity fixing can be difficult under certain conditions. However in this report, we do not cover this field. We focus on measurement accuracy given that the fixed integer values are correct. We assume that no structural variations or systematic errors in the reference network exist. We assume no height variations in the reference network. This effect is described in the section about troposphere influence. We assume that the operator uses the equipment correctly and not introduce additional errors by erroneous handling.

The baseline approach in this paper is to study the use of L1 observations only. All observations are weighted with respect to their elevation angle. The weighing function we use is $sin(\varepsilon)$. Different weighting functions in GNSS processing has been presented, e.g., *Rotacher et al.* [1997], *Jin et al*. [2005]. However, simulations show that the choice of weighting function in network-RTK applications has a rather insignificant impact on the final results. Using the chosen weighting reduces the impact of the tropospheric delay by 10% compared to the use of equal weights. Hence, we have not tried to imitate any specific software in this respect. We use observation above a cutoff angle of 13^o. This value is within the typical range commonly used in GPS processing today. We also assume that the rover estimates 4 parameters, namely its east, north, height coordinates, and its local clock offset to the virtual reference station. The integration time of the observations for the rover is one sample. In our study, we have used a satellite constellation based on GPS and GLONASS during two weeks, from GPS week 1491 and 1492. This is the time period from August 3, 2008 to August 16, 2008. In the paper, we also refer to what we call future GNSS. By that we mean full constellations of GPS, GLONASS, Galileo, and Compass.

Error Modelling

In order to estimate the measurement errors in network-RTK, we need to model the different contributions in (4) and simulate a network with 70 km between the reference stations. The errors in satellite clocks and orbit information will not significantly affect measurements with network-RTK due to the interpolation technique used, see (7). The error in the estimated position due to local clock errors in the receivers is removed in the processing of the GNSS data being one of the estimated parameters; see the section on modelling assumptions. We will thus focus on the errors in the signal delay in the ionosphere, signal delay in the troposphere, and local effects as specified in (4). Below we describe how the covariances of these errors are modelled.

Ionosphere

The ionosphere is the upper part of the atmosphere (approx 100-1000 km) that is ionised by solar radiation. It is a dispersive medium at GNSS frequencies. That is, the refractive index depends on the signal frequency. A consequence of this property is that the GPS signal delays on L1 and L2 are different. Hence a technique to remove a large part of the contribution from the ionosphere is to

form a linear combination of the L1 and L2 phase observables φ_{L1} and φ_{L2} usually referred to as the L3 combination [e.g., *Hoffman-Wellenhof et al*, 1994]

$$\varphi_{L3} = c_1\varphi_{L1} + c_2\varphi_{L2} \tag{8}$$

where c_1 and c_2 are approximately 2.55 and -1.55 respectively. Another common practice is to use the L1 phase observable only which is suitable for short baselines where ionospheric variations to a large extent are cancelled when differencing observations from rover and reference receivers. We model the error contribution from the ionosphere $\Delta\ell_i$ on the observations of *n* simultaneously visible satellites by describing a diagonal covariance matrix

$$\operatorname{cov}\left(\Delta\ell_i\right) = \begin{pmatrix} \sigma_{i1}^2 & 0 & \cdots & 0 \\ 0 & \sigma_{i2}^2 & \cdots & 0 \\ \vdots & \vdots & \ddots & \vdots \\ 0 & 0 & \cdots & \sigma_{in}^2 \end{pmatrix} \tag{9}$$

where the diagonal elements are

$$\sigma_{ik}^2 = \sigma_{io}^2 m_{ik}^2 \frac{1}{f^4} d^{\alpha} \qquad \{k = 1,2,\ldots,n\} \tag{10}$$

where d is the distance between the reference stations in our network configuration (see the section on models assumptions), f is the signal frequency, n is the number of satellites and m_i is the ionospheric mapping function [*Klobuchar*, 1996]

$$m_i = \frac{R + h}{\sqrt{(R+h)^2 - R^2 \sin^2(\theta + \pi/2)}}$$

where *R* is the radius of the Earth, θ is the elevation angle, and we assume that the ionosphere is a thin layer at a height, *h*=400 km. This model of the ionospheric error contribution fits reasonably well with GPS data from Scandinavia from the years 2003 and 2008 [*Emardson et al.*, 2009]. Using this data set, we find the value 2 for α . The parameter σ_{io} varies significantly with time. In the calculations presented in this paper we use a mean value, $2.64 \cdot 10^{11}$ Hz^2, obtained over the years 2003 and 2008. We use this model for distances up to a few hundred kilometres.

Troposphere

The troposphere is the lower part of the atmosphere, usually below 10 km. For simulation purposes we divide the signal delay contribution from the troposphere into two parts, namely a hydrostatic part and a wet part, which is the delay component due to water vapour.

Hydrostatic delay

The hydrostatic delay is larger than the wet delay. It is approximately 2 m in the zenith direction. It is, however, relatively easy to suppress due to very strong horizontal spatial correlation. The vertical hydrostatic delay is almost perfectly correlated with the local atmospheric pressure [e.g.,

Saastamoinen, 1972]. A relatively strong pressure gradient of say 4 mbar over a distance of 100 km results in a difference in the zenith delay of 10 mm over the same distance. This delay gradient is relatively smooth as it follows the pressure gradient and hence a linear combination such as (3) cancels this effect almost completely.

When the reference stations and the rover or a virtual reference station are at different heights, the hydrostatic delay difference has to be taken into account. A combination of large height and temperature differences between reference and rover locations may result in slightly incorrect rover position estimates. We have not included this effect further in the analysis in this paper. However, for geographical areas with large topographical variations this effect should be taken into consideration.

Wet delay

The wet delay is much smaller than the hydrostatic delay, typically below 30 cm in the Nordic countries. However, because of its relatively high spatial and temporal variability it is usually a more serious error source in GPS applications. Because the signal delay in the troposphere is relatively close to the surface, the delays of the signals from the different satellites are correlated, in difference to the ionospheric delay. We model the covariance of the error contribution by using a model for the spatial distribution of its refractivity component, the wet refractivity χ. By using structure functions, D_χ of the wet refractivity, we can express the covariances of the slant wet delay as [*Emardson et al.*, 2009]

$$\begin{aligned}\operatorname{cov}\left(\Delta \ell_t\right) = \tfrac{1}{2} m^i m^j \iint [-D_\chi(r_1^i(v), r_1^j(v')) + D_\chi(r_1^i(v), r_2^j(v')) + \\ + D_\chi(r_2^i(v), r_1^j(v')) - D_\chi(r_2^i(v), r_2^j(v'))] dv dv'\end{aligned} \tag{11}$$

for station 1 and 2 and the signals from satellite *i* and *j* respectively, where

m^k is the wet mapping function [*Niell*, 1997] to satellite k and the integration is performed along the local verticals at the two stations. The wet refractivity structure function for two locations *A* and *B* with position vectors, r_A and r_B, can be modelled as:

$$D_\chi(r_A, r_B) = C_\chi^2 \cdot d_{AB}^{\alpha} \tag{12}$$

when the vertical components v_A and v_B of r_A and r_B are both <1000 m. Otherwise $D_\chi = 0$. Here d_{AB} is the distance between *A* and *B*.

We use the values $\alpha = 0.9$ and $C_\chi^2 = 5.57 \cdot 10^{-15}\, m^{-0.9}$. [e.g., *Treuhaft and Lanyi*, 1987, *Jarlemark*, 1997, *Nilsson*, 2008] in the simulations in this paper.

As seen in (11), the covariance is expressed for the situation with a rover and one reference station, i.e., station 1 and 2 in (11). An expression for a reference network which is based on weighted sums of the covariances in (11) can be found in *Emardson et al.* [2009].

Local Effects

As for the effect of the ionosphere, we can use information obtained at several frequencies in order to mitigate the local effects. A linear combination, L_a, formed in order to reduce the local antenna and environmental effects can be written as [*Emardson and Jarlemark,* 2009]

$$\varphi_{La} = 0.61\varphi_{L1} + 0.39\varphi_{L2} \tag{13}$$

The weighting of the observables L1 and L2 are chosen so that this combined observable L_a can be useful when the contribution from the ionosphere is relatively small and the local effects are relatively large. We can also form a linear combination, L_o, which minimises the combined effect of the ionosphere and the local effects.

$$\varphi_{Lo} = 1.73\varphi_{L1} - 0.73\varphi_{L2} \tag{14}$$

In our simulations, we model the error contribution from the local effects as a diagonal covariance matrix

$$\mathrm{cov}\left(\Delta\ell_e\right) = \begin{pmatrix} \sigma_{e1}^2 & 0 & \cdots & 0 \\ 0 & \sigma_{e2}^2 & \cdots & 0 \\ \vdots & \vdots & \ddots & \vdots \\ 0 & 0 & \cdots & \sigma_{en}^2 \end{pmatrix} \tag{15}$$

where the diagonal elements are:

$$\sigma_{ek}^2 = \sigma_{eo}^2 m_{ek}^2 \qquad \{k = 1,2\ldots.,n\} \tag{16}$$

and we use σ_{eo} equal to 2.1 mm for L1 observations and 2.6 mm for L2 observations [*Emardson et al.*, 2009]. These values are of the same order as values published by *Mader* [1999] based on GPS antenna calibrations. We use m_{ek} equal to *1/sin(θ_k)* for observations at an elevation θ_k.

Error Propagation

The different error sources described in the previous sections will affect the vertical and horizontal coordinates of the estimated position depending primarily on their elevation dependence. In order to determine how much the different error sources contribute to the errors we use the model

$$\mathbf{z} = \mathbf{H}\mathbf{x} + \mathbf{v} \tag{17}$$

Here the vector $\mathbf{z}$ contains the measurement errors due to the ionosphere, troposphere, and local effects. This vector can be formed as different combinations of the observables at the L1 and L2 frequencies. In this paper, we model L1 only observations for the basic scenario. We have also used the combinations L3 and L_o from (8) and (14) respectively. The vector $\mathbf{x}$ contains the parameters we want to estimate, and these are the rover position in three dimensions and a receiver clock offset. The matrix $\mathbf{H}$ contains the partial derivatives matching the estimates with the measurement errors, and primarily depends on the satellite constellation used, see the section on modelling assumptions.

In our simulations, we have processed the data with 1 minute intervals except for the troposphere that we update once per hour. We have used an elevation cutoff angle of 13^{o} and the observations are weighted with $w=\sin(\theta)$, see the section on modelling assumptions. Using this weighting, we form $\mathbf{W}$ as a diagonal matrix with the values w on the diagonal. Using this modelling approach, we could generate random errors based on the statistical representation of the errors. We have chosen, however, to calculate the errors in the estimated parameters as:

$$\mathrm{cov}(\hat{\mathbf{x}}) = (\mathbf{H}^T\mathbf{W}\mathbf{H})^{-1}\mathbf{H}^T\mathbf{W}\,\mathrm{cov}(\mathbf{z})\mathbf{W}^T\mathbf{H}\left(\mathbf{H}^T\mathbf{W}\mathbf{H}\right)^{-1} \quad (18)$$

In this paper, we assume the error contributions are uncorrelated. Hence we can write

$$\mathrm{cov}(\mathbf{z}) = \mathrm{cov}(\Delta\ell_i) + \mathrm{cov}(\Delta\ell_t) + \mathrm{cov}(\Delta\ell_e) \quad (19)$$

and simulate the different error contributions separately.

Results

Current Situation

We can now summarize and quantify the various error sources that affect the quality of the measurements with network-RTK. In this paper we focus on the vertical coordinate of the estimated positions. For a typical satellite constellation for the period in 2008 and normal atmospheric conditions we get a 1-sigma error in the vertical coordinate of the estimated position, which is 27 mm. This error is based on modeling measurements made on the L1 frequency. Figure 1 shows the contributions to this total error from three different error sources, ionosphere, troposphere, and local effects. The contributions from the ionosphere and troposphere dominate, with troposphere contribution slightly larger than that from the ionosphere. We must be aware that the contribution of the ionosphere will increase as we get closer to next solar maximum around 2012. A method for reducing the contribution from the ionosphere is to use the L3 combination of the L1 and L2 observables from (8). This combination is largely insensitive to variations in the ionosphere. In the figure are also the contributions from the three error sources from the L3-use. The total error in the vertical coordinate is still about 27 mm. However, the contribution from the ionosphere is reduced to virtually zero. However, this has been at the expense of the local errors, which is now a significant error contribution of the same magnitude as the contribution from the troposphere. In many RTK processing systems a combination of the L1 and L2 observable are used. We illustrate this using the L_o observable from (14). Results using this combination are shown in the figure with blue bars. It is clear from the figure that the contribution from the troposphere is not affected by the choice of observable combination due to its non-dispersive effect on the GNSS signals.

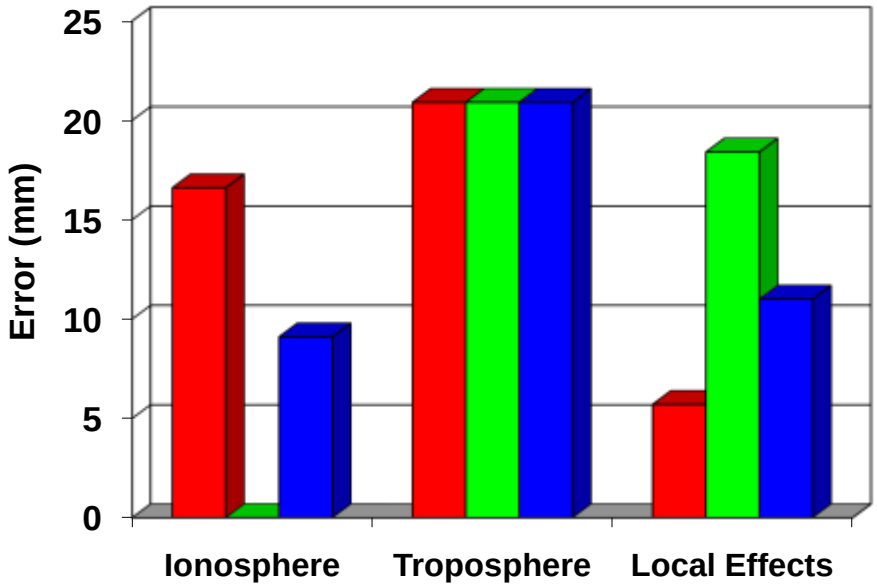

Figure 2 Error contribution from the three error sources for for L1 (red), L3 (green), and L_o (blue) processing.

Future Situation

Based on the modeling described above, we can predict the accuracy we can attain using systems under development and by a densification of the reference network. Figure 2 shows the estimated error components in network RTK for a few different scenarios. These are (1) the current situation as described in previous sections with a reference station interdistance of 70 km, (2) the availability of future GNSS constellations, (3) a densification of the reference network to 35 km, and (4) a combination of (2) and (3). As we explained above, we have an error in the estimated vertical coordinate of about 27 mm with the current situation. The access to new GNSS reduces this error to about 20 mm. Approximately the same effect is obtained from a densification of the reference network to 35 km between the reference stations. A combination of both would reduce errors down to 13 mm in the vertical coordinate.

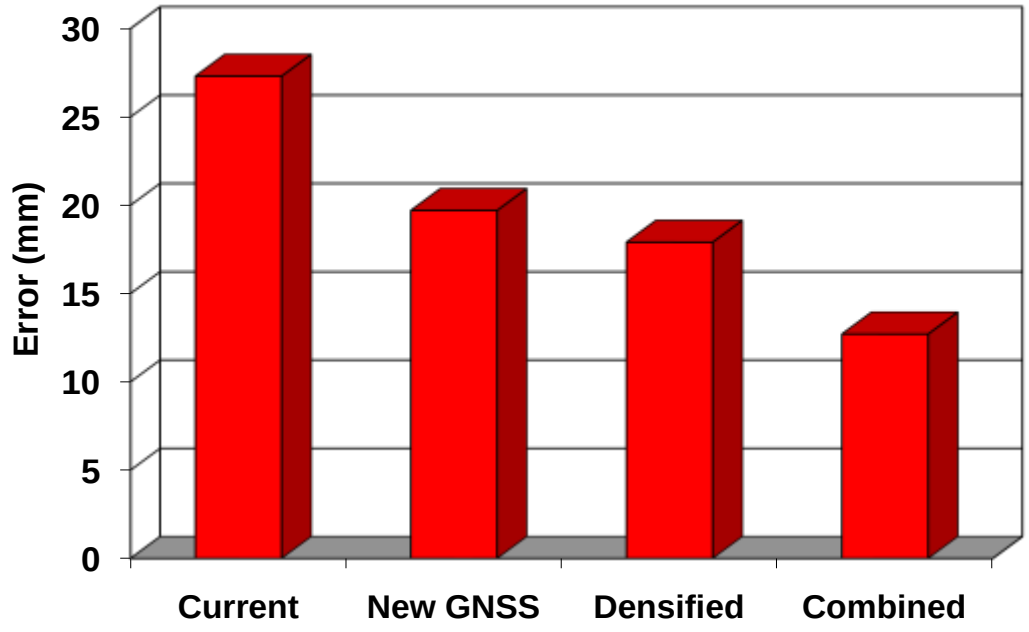

Figure 3 **Errors in network RTK for different scenarios all based on L1 processing only.**

Studying the various scenarios in more detail, we can see the size of the different error contributions. Figure 4 shows the error contribution from the three error sources ionosphere, troposphere and the local effects for the current situation. The figure also show the presumed results when we have access to new GNSS. These results are displayed for cutoff angle of both 13^{o} and 25^{o}. Using a higher cutoff angle results in a slightly better accuracy when more satellites are available than today. New GNSS provides, compared with the current configuration, a reduction in the error contribution from the ionosphere and the local effects. The contribution from the troposphere is not affected. However, if we raise the elevations-cutoff-angle to say 25^{o}, the contributions are somewhat redistributed. The contribution from the ionosphere increases compared to when using the lower cutoff angle. The contribution from the troposphere, however, decreases when we increase the cutoff angle. The contribution from the local effects is largely unchanged. The total error in the

estimated vertical coordinate is about 20 mm when we have access to new GNSS.

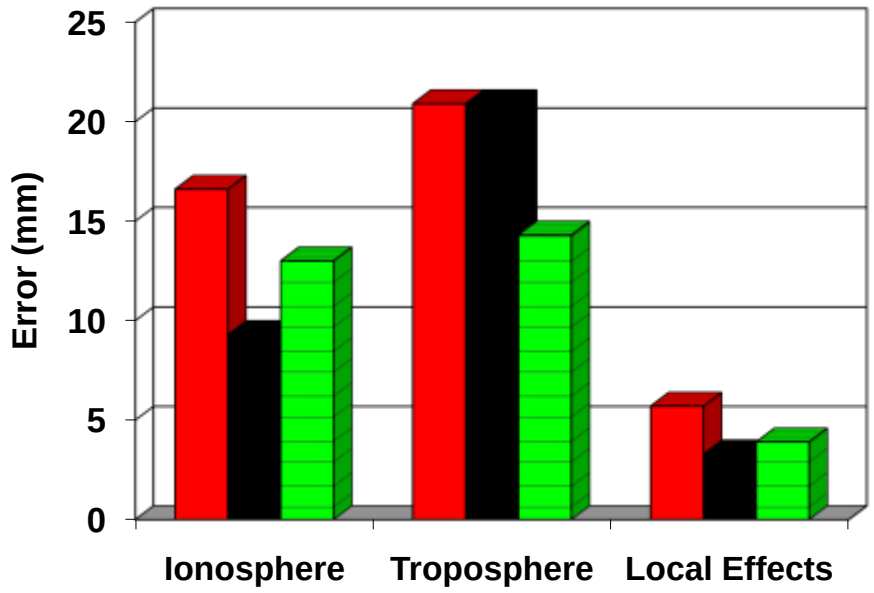

Figure 4 **Error contribution from the three error sources for nominal (red), new GNSS with an elevation cutoff of 13° (black), and new GNSS with an elevation cutoff of 25° (green striped). Results are based on L1 processing only.**

As shown in Figure 3, the overall results from the availability of new GNSS and from a densified reference network are relatively similar. We can now study the separate error contributions for these scenarios. Figure 5 shows the error contributions from the three error sources ionosphere, troposphere and the local effects at the current situation, with access to new GNSS and a densified network of 35 km between reference stations. The overall errors are about 20 mm for both new GNSS and for a densified reference network. The advantage with a densified reference network, compared to access to new GNSS, is in the reduced contribution from the ionosphere. Also the contribution of the troposphere is reduced compared with the current situation, although not as much as when we have access to new GNSS. The error contribution from the local effects is not affected by a densification of the reference network.

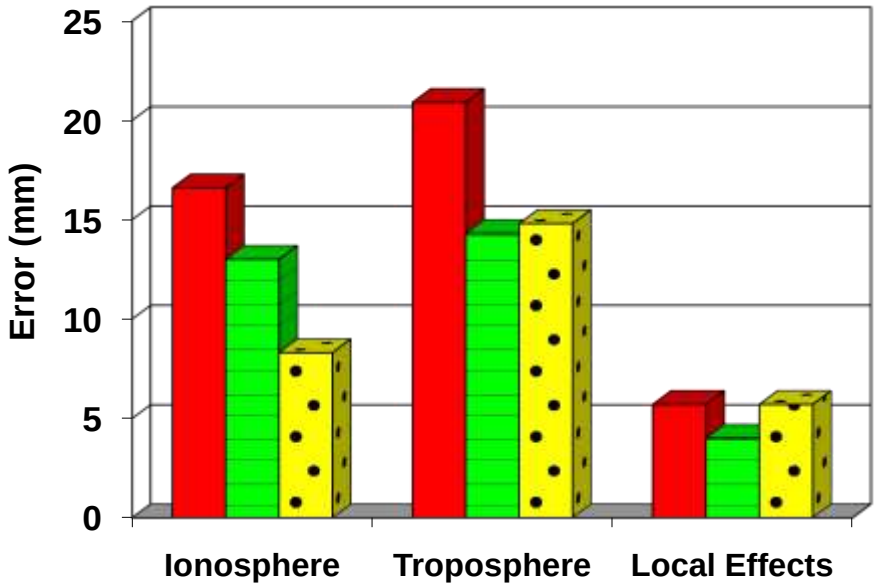

Figure 5 Error contribution from the three error sources for nominal (red), new GNSS (green striped), and densified network (yellow dotted).

Conclusions

We have studied the expected uncertainty from measurements with network-RTK by modeling the contribution error sources. For standard Scandinavian conditions and a reference network with 70 km between the reference stations, we find an uncertainty in the vertical coordinate of a measured position of 27 mm. The introduction of future satellite systems such as Galileo and Compass with for the user a greater availability of transmitting satellites can reduce the error from the present 27 mm to 20 mm using the same reference network. With more transmitting satellites, a higher cutoff angle may be beneficial. A densified reference network of 35 km between reference stations provides a similar improvement in performance as the availability of new satellite systems, i.e., a reduction in the error from 27 mm to 18 mm. Using both a densified network and the new satellite systems reduces the error in the estimated vertical coordinate further down to 13 mm. Periodically, the contribution of the ionosphere can be assumed to be a dominant error sources in network-RTK. For those periods it is important to consider the trade-off between suppressing the effect from the ionosphere and suppressing the local effects.

References

Emardson T.R., and P.O.J. Jarlemark, Optimal linear combinations of GNSS observables, *in preparation for GPS solutions*, 2009.

Emardson T.R., Jarlemark, P.O.J, Bergstrand S., Nilsson T., and Johansson J., Measurement Accuracy in Network-RTK, SP report 2009:23, ISBN 978-91-86319-10-6, 2009.

Hoffman-Wellenhof B., H. Lichtenegger, and J. Collins, GPS: Theory and practice, *Springer Verlag, New York,* 1994.

Jin, S. and Wang, J. and Park, P.H., An improvement of GPS height estimations- Stochastic modeling, Earth, Planets, and Space, 4, 253--259, 2005.

Klobuchar J.A., Ionospheric Effects on GPS, in *Global Positioning System: Theory and Applications*, *1*, eds: B. W. Parkinson and J. J. Spilker, pp. 485-514, 1996.

Landau, H., Vollath, U. and Chen, X., Virtual reference station systems, Journal of Global Positioning Systems, 1, 137-143, 2002.

Lim, S. and Rizos, C., A Conceptual Framework for Server-Based GNSS Operations, Journal of Global Positioning Systems, 7, 125-132, 2008.

Mader G.L, GPS Antenna Calibration at the National Geodetic Survey, GPS Solutions, 3, 50-88, 1999, DOI - 10.1007/PL00012780.

Niell A.E., Global Mapping Functions for the Atmospheric Delay at Radio Wavelengths, J. Geophys. Res., 101, 3227-3246, 1996.

Nilsson T., Measuring and modelling variations in the distribution of atmospheric water vapour using GPS, *PhD thesis, Chalmers Univ of Tech.*, 2008.

Rizos, C. and Han, S., Reference station network based RTK systems-concepts and progress, Wuhan University Journal of Natural Sciences, 8, 566—574, 2003

Rothacher, M. and Springer, T.A., Schaer, S., and Beutler, G., Processing strategies for regional GPS networks, Advances in positioning and reference frames: IAG Scientific Assembly, Rio de Janeiro, Brazil, September 3-9, 1997.

Saastamoinen J., Atmospheric corrections for the troposphere and stratosphere in radio ranging of satellites, *The use of artificial satellites for Geodesy, Geophys. Monogr. Seriesvol 15*, ed: S. W. Henriksen et al, pp. 247-251, AGU, Washington, D. C., 1972.

Treuhaft R.N., and G.E. Lanyi, The effects of the dynamic wet troposphere on radio interferometric measurements, *Radio Sci., 22*, pp. 251-265, 1987.